THEORETICAL AND EXPERIMENTAL INVESTIGATION OF HIGH-LATITUDE OUTFLOW FOR IONS AND NEUTRALS

Larry C. Gardner and Robert W. Schunk

Center for Atmospheric and Space Research
Utah State University
Logan, UT 84322

Abstract

The outflow of ions at high latitudes is one mechanism thought to populate the magnetosphere with ionospheric ions [H^+, He^+, O^+]. Computer modeling can give an insight into the mechanisms and rates at which these ions can populate the magnetosphere, but for atomic oxygen the temperature is about 40% lower than measurement. This can be accounted for by the inclusion of a hot O population at a higher temperature, of about 4000K.

Polar Wind

The sun emits a continuous, yet variable, flow of plasma, which moves radially away for the sun's surface, and is known as the solar wind. Due to the high conductivity of the plasma in the solar wind, the magnetic field of the sun is "frozen-in" or dragged along with the outflowing solar wind, and thus forms a spiral structure due to the rotation of the sun. As the speed of the solar wind changes over time, fast flow streams may overtake slow flow streams and shock waves can be produced, which can impact the Earth (see Figure 1).

As the solar wind flows through interplanetary space, it has to pass the orbit of the Earth. Therefore, the solar wind impacts the Earth, and the Earth would loose its atmosphere were in not

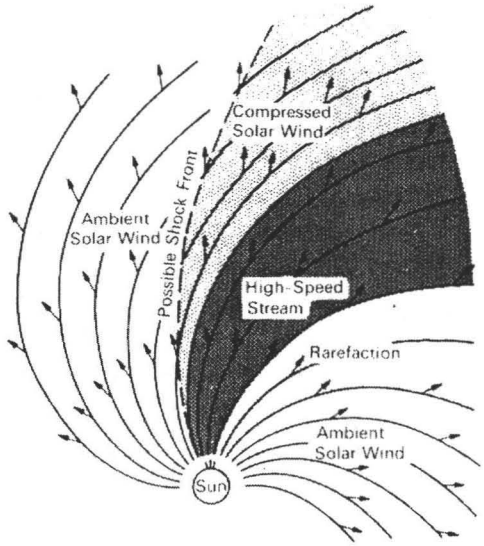

Figure 1. Graphic showing the production of shocks due to variable speed flows, and the spiral structure of the magnetic field (T. E. Holzer, in *Solar System Plasma Physics*, vol. I. North-Holland, 1979, p.103, Elsevier Science Publishers).

for its natural intrinsic magnetic field. The Earth's magnetic field acts as a hard obstacle to the supersonic solar wind, and therefore deflects the solar wind around the Earth. This then produces a bubble – the magnetosphere, in which we live. The magnetic field is thereby compacted on the sunward side of the Earth and stretched out into a long tail, which extends beyond the orbit of the

moon on the anti-sunward side of the Earth (see Figure 2).

Due to the stretched out structure of the magnetic field on the nightside, or anti-sunward side of the Earth, there is a

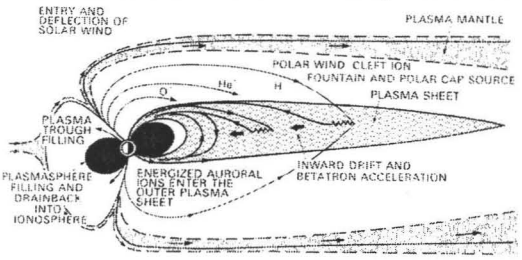

Figure 2. Plot showing the structure of the Earth's geomagnetic cavity (After C. R. Chappell, *Rev. Geophys., 26*, 229, 1988, copyright by the American Geophysical Union).

large pressure differential along these diverging magnetic field lines. This then causes the electrons and lighter ions to diffuse out to higher altitudes. Since the electrons are lighter they diffuse faster, but as they diffuse out there is a slight charge separation between them and the ions, which in turn causes an ambipolar electric field to be set up. This ambipolar electric field in turn causes the ions to be pulled along with the outflowing electrons. This outflow due to diffusion and the pressure gradient is what is termed the classical polar wind, and is named in analogy to the solar wind [*Axford*, 1968].

The polar wind is composed mainly of electrons and thermal ions [H^+, He^+, O^+], which originate in the Earths ionosphere. As the ions flow out along diverging geomagnetic field lines they undergo four major transitions:

(1) Chemical to diffusive equilibrium;
(2) Subsonic to supersonic flow;
(3) Collision-dominated to collisionless;
(4) Heavy to light ion dominance.

Theoretical Model

The model used in this study is a hydrodynamic model, with equations being solved with initial conditions and boundary values using the well-known flux-corrected-transport (FCT) technique [*Borris and Book*, 1976]. The time-dependent continuity and momentum equations are solved for H^+ and O^+ ions along diverging magnetic field lines. The continuity and momentum equations for this study are shown respectively as:

$$\frac{\partial n_i}{\partial t} + \frac{1}{A}\frac{\partial}{\partial r}\left(A n_i u_i\right) = P_i - L_i n_i \tag{1}$$

$$\begin{aligned} &\rho_i\left[\frac{\partial u}{\partial t} + \frac{\partial}{\partial r}\left(\frac{u_i^2}{2}\right)\right] + \frac{\partial}{\partial r}\left(n_i k T_i^{II}\right) \\ &- n_i e_i E_{II} + \rho_i \frac{GM_E}{r^2} \\ &+ n_i k\left(T_i^{II} - T_i^{\perp}\right)\frac{1}{A}\frac{\partial A}{\partial r} \\ &= \rho_i \sum_j \nu_{ij}\left(u_j - u_i\right)\Phi_{ij} \end{aligned} \tag{2}$$

where n_i is the ion density (H^+ or O^+), u_i is the field-aligned drift velocity, T_i^{II} is the temperature in the direction of the magnetic field, $T_i^{\perp}$ is the temperature perpendicular to the magnetic field, m_i is the mass, $\rho_i = n_i m_i$, P_i is the production rate, L_i is the loss frequency, ν_{ij} is the momentum transfer collision frequency for species i and j, Φ_{ij} is a velocity-dependent correction factor, E_{II} is the polarization electric field, e is the electron charge, k is Boltzmann's constant, G is the gravitational constant, M_E is the Earth's mass, t is time, r is the distance along the magnetic flux tube,

and A is the cross-sectional area of a flux tube.

The polarization eletctric field is obtained via the electron momentum equation

$$E_{II} = -\frac{1}{en_e}\frac{\partial p_e}{\partial r} \tag{3}$$

where subscript e is used for electrons, $p_e = n_e k T_e$ where T_e is assumed to be governed by the equation of state

$$T_e n_e^{(1-\gamma_e)} = const \tag{4}$$

with γ_e being the ratio of specific heats.

At low altitudes an isotropic temperature structure is assumed where the parallel and perpendicular ion temperatures are equal. Above 1300 km, the following ion equation of state is adopted

$$T_i n_i^{(1-\gamma_{ii})} = const\,. \tag{5}$$

At high altitudes, the dominant production and loss processes for H^+ and O^+ is the accidentally-resonant charge exchange reaction,

$$O^+ + H \Leftrightarrow O + H^+ \tag{6}$$

where the forward, k_f, and reverse, k_r, reaction rates are given by [cf. *Raitt et al.*, 1975; *Barakat et al.*, 1987]

$$k_r = 2.5\times10^{-11}\left[T_n + \frac{T_{O^+}}{16} + 1.2\times10^{-8}u_{O^+}^2\right]^{\frac{1}{2}} \tag{7}$$

$$k_r = 2.2\times10^{-11}\left[T_{H^+} + \frac{T_n}{16} + 1.2\times10^{-8}u_{H^+}^2\right]^{\frac{1}{2}} \tag{8}$$

where T_n is the neutral temperature and the units are cm^3s^{-1}.

In the momentum equation (2) the H^+ and O^+ ions are assumed to collide with each other and with neutral atomic oxygen and hydrogen. *Raitt et al.* [1975] give the appropriate collision frequencies and velocity-dependent correction factors.

Model Results

The model was run for a time to allow for the solution to reach a steady state. The steady state density profiles are shown in Figure 3 for both H^+ (solid) and O^+ (dashed) with the atomic O and H densities being fixed by the MSIS model and the O^+ and H^+ densities at the boundary [500 km] being controlled by the accidentally-resonant charge exchange reaction shown in (6).

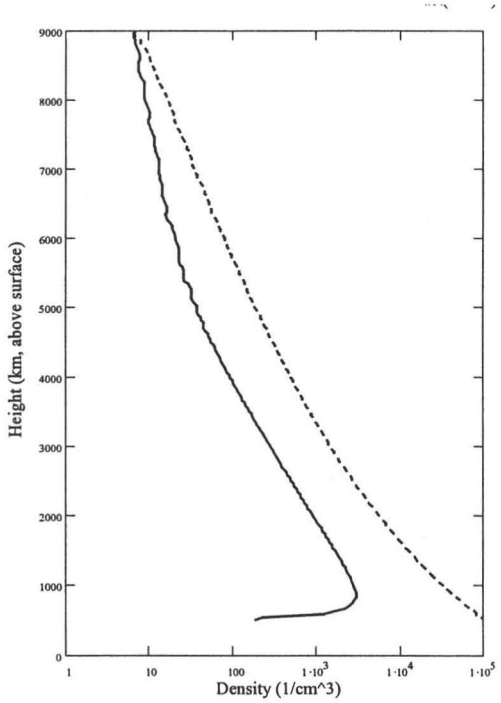

Figure 3. Plot showing the density profiles for H^+ (solid) and O^+ (dashed)

The velocity plots are shown in Figure 4, and show the collective effects of diffusion and collisions. Below approximately 4000 km the H^+ velocity profile is controlled by the slower moving O^+ due to collisions and the fact that gravity holds O^+ stronger than H^+. Above about 4000 km, the collison frequency decreases and thus H^+ is less strongly affected by the O^+ and this allows for an accelerated aoutflow of H^+.

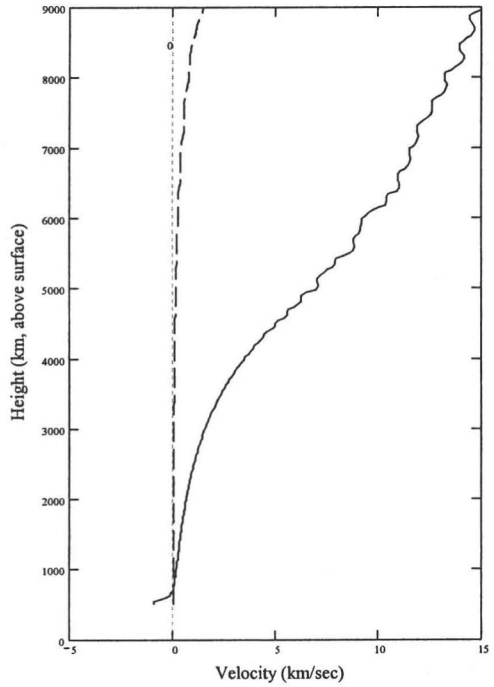

Figure 4. Same as Figure 3, but for velocity.

Hot oxygen

Measurements have shown that a difference between experimental and theoretical O^+ ion temperature exists. The temperature difference can be accounted for by the existence of a hot atomic oxygen population.

The main experimental evidence for the existence of a hot O population is from optical observations of airglow taken at high altitude [*Schoendorf et al.*, 2000]. *Hernandez* [1971] observed fast O in the F region above Jicamarca, Peru; *Yee et al.* [1980] inferred a hot O population from exospheric airglow measurements above Michigan, *Hedin* [1989] estimated hot O from differences between the Mass Spectrometer Incoherent Scatter (MSIS) model and satellite drag models; and *Cotton et al.* [1993] found a hot O population would explain excess UV airglow observed in sounding rocket observations. All of the above results predict about the same thing, a hot O population of 1-2% of the ambient O at 550 km, but do not define a profile shape, other than *Cotton et al.* [1993] which suggests a layer profile.

The F region ions are heated mainly through collisions with warmer electrons, and cooled through collisions with cooler neutrals. This leads to the ion temperature being somewhere between the electron and neutral temperatures, as determined by the electron and ion densities [*Oliver and Schoendorf*, 1999].

Oliver and Glotfelty [1996] looked at data from Milstone Hill between 1970 and 1975 between the hours of 9 and 15 local time. They used the atomic oxygen density from the MSIS model under the assumption that MSIS incorporates actual atomic oxygen density measurements form those years. Thus representing the atomic oxygen density well on average. They found that the ion temperature from theory was lower than measured. They put forth two possibilities, a decrease in ion cooling or an increase in the ion heating (about 40%).

To date, the hot O population has largely been ignored, but the work done suggests a temperature for the hot O population of 4000 K. *Shematovich et al.* [1994] showed that hot O was about 1% of the total O at all altitudes above

300 km. Cold O, however, thermally quenches hot O, and higher thermal O densities lead to lower hot O densities. This would then suggest, as in *Cotton et al.* [1993], a chapman-type layer peaked near the exobase, with a sharp bottom side and a topside which approaches diffusive equilibrium toward higher altitudes with a scale height appropriate for O at 4000K (see Figure 5).

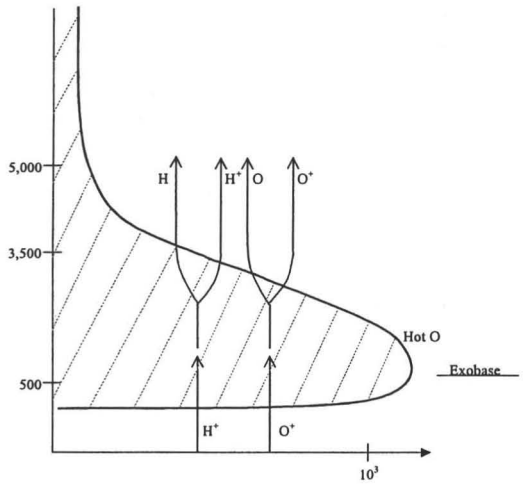

Figure 5. Plot showing the expected layer profile for the hot O population and the suspected charge exchange mechanism.

Conclusions

This study has incorporated an FCT method developed by Borris and Book [1976] to solve the time dependent continuity and momentum equations for H^+, and O^+ atoms being controlled by the accidentally-resonant charge exchange reaction (6). It is found that the density profile for H^+ shows the production of H^+ from the charge exchange at low altitudes with the profile approaching a maximum with increasing altitude. The O^+ density profile shows that O^+ approaches diffusive equilibrium for all altitudes considered. The velocity profile for H^+ shows the dependence of velocity on the collision frequency with O^+, with the profile showing a slow decrease in velocity at low altitudes due to collisions and an exponential increase as collisions become less important. The O^+ velocity profile shows that the O^+ is more gravitationally bound than H^+ with the profile only slowly increasing with height.

The velocity profiles, however, are about 40% lower than measurement shows. This can be explained by a hot O profile with a temperature of 4000K. This effect will be examined in the future with the model being adapted to include the effects of the hot O population and then the appropriate hot O profile can then be determined.

References

Axford, W. I., The polar wind and the terrestrial helium budget, *J. Geophys. Res.*, *73*, 6855, 1968.

Barakat, A. R., and R. W. Schunk, Stability of the polar wind, *J. Geophys. Res.*, *92*, 3409, 1987.

Borris, J. P., and D. L. Book, Solution of continuity euations by the method of flux-corrected transport, in *Methods in Computations Physics,* vol. 16, edited by B. Alder, s. Fernbach and M. Rotenberg, pp. 85-129, Academic, San Diego, Calif., 1976.

Cotton, D. M., G. R. Gladstone, and S. Chakrabarti, Sounding rocket observation of a hot oxygen geocorona, *J. Geophys. Res.*, *98*, 21,651-21,657, 1993.

Heden, A. E., Hot oxygen geocorona as inferred from neutral exospheric models and mass spectrometer measurements, *J. Geophys. Res., 94*, 5523-5529, 1989.

Hernandez, G., The signature profiles of $O(^1S)$ in the airflow, *Planet. Space Sci., 19*, 467-476, 1971.

Oliver, W. L., and K. Glotfelty, O^+-O collision cross section and long-term F region O density variations deduced from the ionospheric energy budget, *J. Geophys. Res., 101*, 21,769-21,784, 1996.

Oliver, W. L., and J. Schoendorf, Variations of hot O in the thermosphere, *Geophys. Res. Lett., 26*, 2829-2832, 1999.

Raitt, W. R., R. W. Schunk, and P. M. Banks, A comparison of the temperature and density structure in the high and low speed thermal proton flows, *Planet. Space Sci., 23*, 1103, 1975.

Schoendorf, J., L. A. Young, W. L. Olover, Hot oxygen profiles for incoherent scatter radar analyis of ion energy balance, *J. Geophys. Res., 105*, 12,823-12832, 2000.

Shematovich, V. I., D. V. Gisikalo, and J. C. Gérard, A kinetic model of the formation of the hot oxygen geocorona, *J. Geophys. Res., 99*, 23,217-23,228, 1994.

Yee, J. H., J. W. Meriwether Jr., and P. B. Hays, Detection of a corona of fast oxygen atoms during solar maximum, *J. Geophys. Res., 85*, 3396-3400, 1980.